Materials Research Proceedings 44 (2024) 475-481 https://doi.org/10.21741/9781644903254-51

Residual stress and part distortion prediction in L-PBF of Ti-6Al-4V using layer-by-layer FEM simulation

POLLARA Gaetano[1,a*], PALMERI Dina[1,b], BUFFA Gianluca[1,c] and FRATINI Livan[1,d]

[1]Dipartimento di Ingegneria, Università Degli Studi di Palermo, Viale delle Scienze, Palermo, 90128, Italy

[a]gaetano.pollara@unipa.it, [b]dina.palmeri@unipa.it, [c]gianluca.buffa@unipa.it, [d]livan.fratini@unipa.it

Keywords: Numerical Simulation, Laser Powder Bed Fusion, Ti-6Al-4V

Abstract. Due to its ability to accommodate customer demands and produce objects with complex shapes, Laser Powder Bed Fusion (LPBF) has been widely adopted in numerous industry areas, including biomedical, automotive, and aerospace. Even with all the benefits that LPBF has to offer, its use may be limited by the development of residual stress according to the strong thermal gradients produced throughout the process. Residual stresses within the samples can result in part distortion after the removal from the built platform or even in part failure during the process if the residual stresses are excessive. In order to save time and costs, numerical simulation can be an effective tool to predict residual stress and part distortion in opposition to the trial-and-error approach which involves an expansive and time-consuming experimental campaign. To this aim a finite element method (FEM) together with a layer-by-layer approach was used in this study. Numerical simulations were performed on the commercial software DEFORM-3D™ with which different values of laser power were investigated. Moreover, the influence of the voxel mesh on the FEM model accuracy was also investigated.

Introduction

Laser power bed fusion (L-PBF) thanks to the possibility to produce complex shapes and to obtain highly customized products, is widely adopted in the aerospace, automotive, and biomedical industries [1]. L-PBF is mostly adopted in the case of metallic components, especially for the production of Ti-6Al-4V parts that can be difficult to work with traditional manufacturing technology. Moreover, Ti-6Al-4V is widely used in aerospace and biomedical applications thanks to its higher strength, low density, and high corrosion resistance [2]. Due to the high thermal gradients and cooling rates developed during the process, residual stresses are usually presented in the produced part at the end of the process [3]. Depending on the amount of residual stresses generated in the L-PBF process, distortion of the part or job failure can occur due to the collision of the warped part with the recoater [4,5]. The trial-and-error approach is not suitable for this technology due to the elevated production time and materials costs [6]. For this reason, numerical simulation can help predict the outcome of the printing process in terms of residual stress and part distortion in order to save time and money [7]. There are many numerical simulation approaches depending on the scale of the problem being issued. The microscale approach can be used when the study is focused on process parameters optimization and the scope is to analyze the behavior of the melt pool. In this case, a Computational Fluid Dynamics (CFD) numerical method is preferred [8]. In the mesoscale approach, one or more hatches are deposited simultaneously. In this way, it is possible to study the effect of the scan strategy on the residual stress distribution within the layer [9]. When the aim is to analyze the macroscopic effect of the process parameters, a part-scale approach is usually adopted in which one or more layers are heated up together. This approach allows for shortening the computational cost and so the simulation time [10].

In this paper, a Finite Element Method (FEM) was used for predicting residual stress and part distortion of Ti-6Al-4V parts during the L-PBF process. In detail, the effect of laser power on residual stress and part distortion was investigated. Moreover, the influence of the voxel mesh and the number of computational layers on the model accuracy was also analyzed. The results of this study can help engineers in the design phase for the L-PBF process of Ti-6Al-4V alloy.

FEM model and experimental details

Numerical model. In this study, a Finite Element Method (FEM) was used for predicting residual stress and part distortion of Ti-6Al-4V parts during the L-PBF process. To this aim, FEM analyses were carried out through the commercial software DEFORM-3D™ v12.0 (V12.0, SFC, Columbus, OH, USA) in which a part-scale approach was adopted. In the part-scale approach, the power input is applied to the whole layer simultaneously and can be expressed as:

$$\dot{q} = \frac{\eta P}{V_{pool}} \quad (1)$$

Where η is the laser efficiency, P is the laser power [W], and V_{pool} is the heat-affected volume. In detail, V_{pool} represents the elements being activated by the heat source in the considered time step [11]. The elements are activated according to the born-dead-elements technique in which the elements affected by the heat source are identified through a search algorithm depending on the used voxel mesh. The reader can refer to [12] for further details regarding the voxel mesh. The dog bone geometry of external dimensions equal to 46 x 8 x 3 mm^3 and was designed in Autodesk Fusion 360 and the STL file was imported in DEFORM-3D™ v12.0 (Fig. 1).

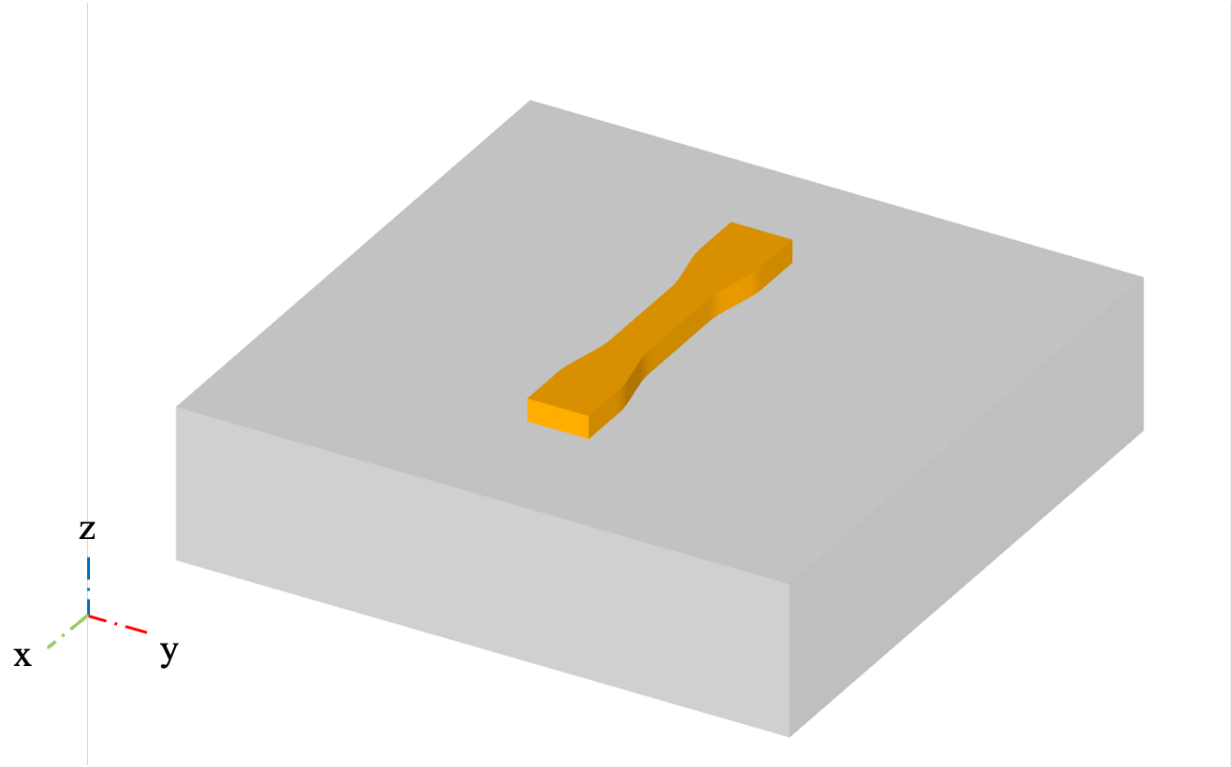

Fig. 1. Sample geometry used in this study to evaluate part distortion in L-PBF.

The specimen was placed on a build plate of 80 x 80 x 25 mm^3 with which sticking conditions were applied in order to avoid detachment during the simulation of the printing process. The build chamber and the build plate temperatures were set at 40°C and 200°C, respectively. Only the heat exchange with the argon was considered in the numerical model (h_{conv} = 1 W/m2 °C) to reduce the

calculation time. The thermomechanical problem was solved with a 12th Gen Intel (R) Core (TM) i9-12900 2.40 GHz processor by using a Newton-Rapson iteration coupled with a MUMPS (MUltifrontal Massively Parallel Sparse) solver. In this study, three different values of laser power were investigated by using three voxel mesh dimensions to investigate their effect on the model accuracy. Particularly, the voxel mesh dimension on the XY plane was kept constant and equal to 0.4 x 0.4 mm^2, while the dimension along the thickness of the sample was varied by using 5, 10, 15 and 20 elements for the voxel meshes v_z=5, v_z=10, v_z=15 and v_z=20 respectively. In this way, the voxel mesh along the Z-direction will result in 0.6 mm, 0.3 mm, and 0.15 mm for v_z=5, v_z=10, v_z=15 and v_z=20 respectively. As a consequence, by considering a layer thickness of 60 μm, the number of real layers in the computational one will be equal to 10 for v_z=5, 5 for v_z=10, 3.3 for v_z=15 and 2.5 for v_z=20.

Experimental Details. Numerical simulations were validated through an experimental campaign where samples with three different values of laser power (300W, 350W, and 400W) were fabricated with an SLM280HL 3D printing machine using Ti-6Al-4V spherical powder with a Gaussian size distribution of 20–63 μm and mass density of 4.43 g/cm3. During the L-PBF process of the dog bone specimens the build orientation, hatch distance (h), scan strategy (s), and layer thickness (l_t) were kept constant and equal to 0°, 100 μm, 0°, and 60 μm, respectively. The oxygen level during the printing process was maintained lower than 1% by filling the build chamber with argon. Moreover, in order to minimize the build-up of residual stress during the printing process, the platform was preheated up to 200 °C.

To validate the result from the numerical simulation, the CAD model of the dog bone specimen geometry was compared to the acquired printed geometry after the removal from the build platform. In detail, the printed geometry was acquired according to the fringe projection approach through a 3D COMET V system (Steinbichler, Neubeuern, Germany). In this way, it was possible to measure the difference between the CAD model and the acquired printed geometry in terms of the Z-direction displacement of the top right corner (Fig. 2).

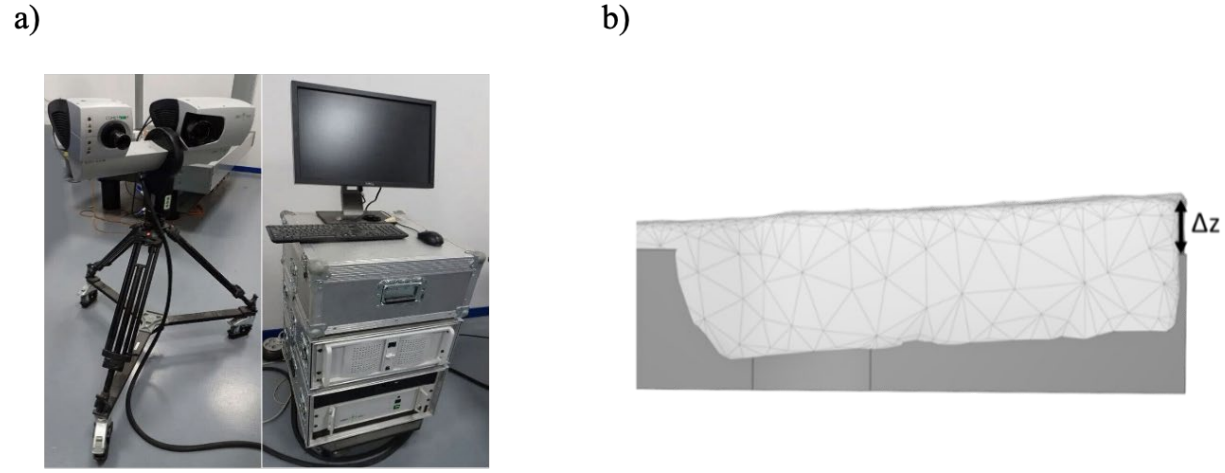

Fig. 2. Distortion measurement a) 3D acquisition system and b) comparison between the CAD model and the acquired geometry in terms of Z-displacement (Δz).

This value was compared with the Z displacement of the top right corner obtained with the numerical simulations.

Results and discussion

The accuracy of the numerical model, by varying the voxel mesh simulation, was investigated. To this aim, real distortions in terms of Δz displacement of the top right corner of the sample were

measured as previously explained. The results from the real distortion measurements are shown in Fig. 3 together with the simulated values obtained with different voxel mesh elements and laser power values.

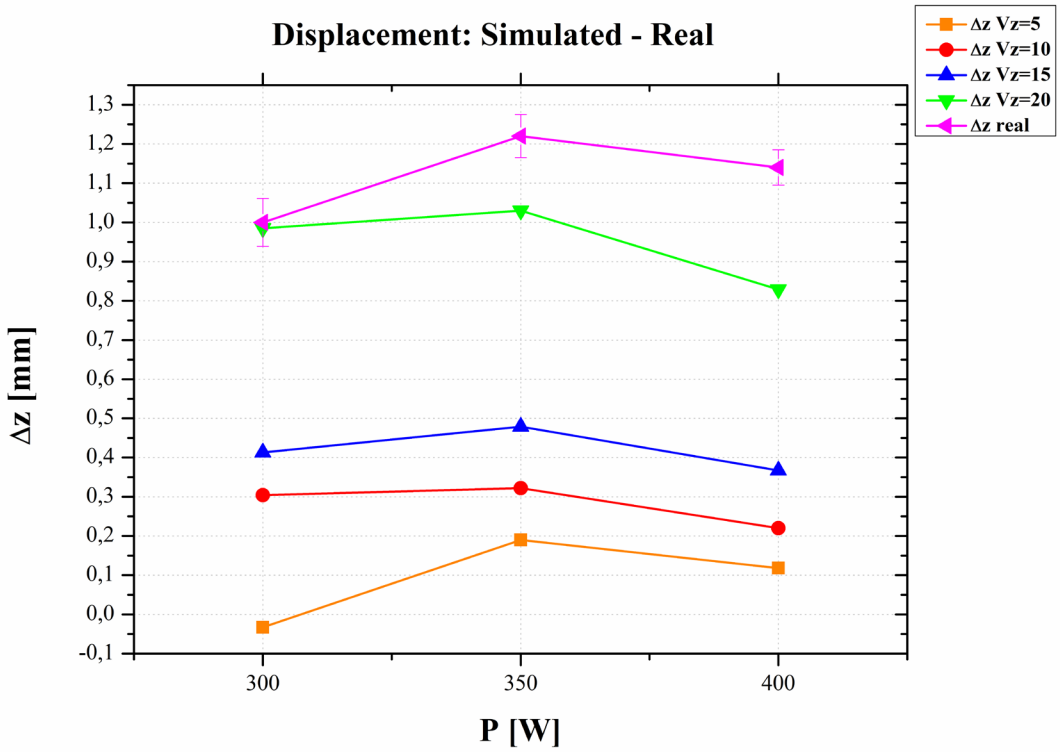

Fig. 3. Distortion measurements from numerical simulation with different voxel meshes (v_z=5, v_z=10, v_z=15 and v_z=20) compared to experimental ones (Δz real).

It can be observed, for the real distortion measurements, how they first increase by increasing the laser power and then decrease. In detail, for laser power below P = 350 W, there is an increase in the thermal gradients, along the build direction (z), that directly affects the residual stress profiles and distortion. For laser power higher than 350 W it can be noted how the gradient of residual stress, along the build direction (z), is lower than that one for the P = 350 W. This is because of the greater remelting area interested by the higher value of laser power as shown in the temperature profiles obtained with the numerical simulations (Fig. 4). Moreover, this laser power value can result in gas porosity acting as a stress relief factor.

By considering the distortion values shown in Fig. 3, for different voxel mesh elements along the z-direction (v_z), it can be stated that for v_z = 20 it is possible to have the best accuracy of the numerical simulation, especially for P = 300 W. Overall, by increasing v_z from 5 to 20 the accuracy of the FEM model increases. This is because increasing the number of voxel mesh elements along the z-direction means reducing the number of real layers embodied in the computational one. Using a few elements, as in the case of v_z = 5, is not enough to well approximate the L-PBF process when a sample of the geometry used in this study is considered. In this case, where a layer thickness of 60 μm is adopted, using a v_z = 5 means including 10 real layers in the computational ones.

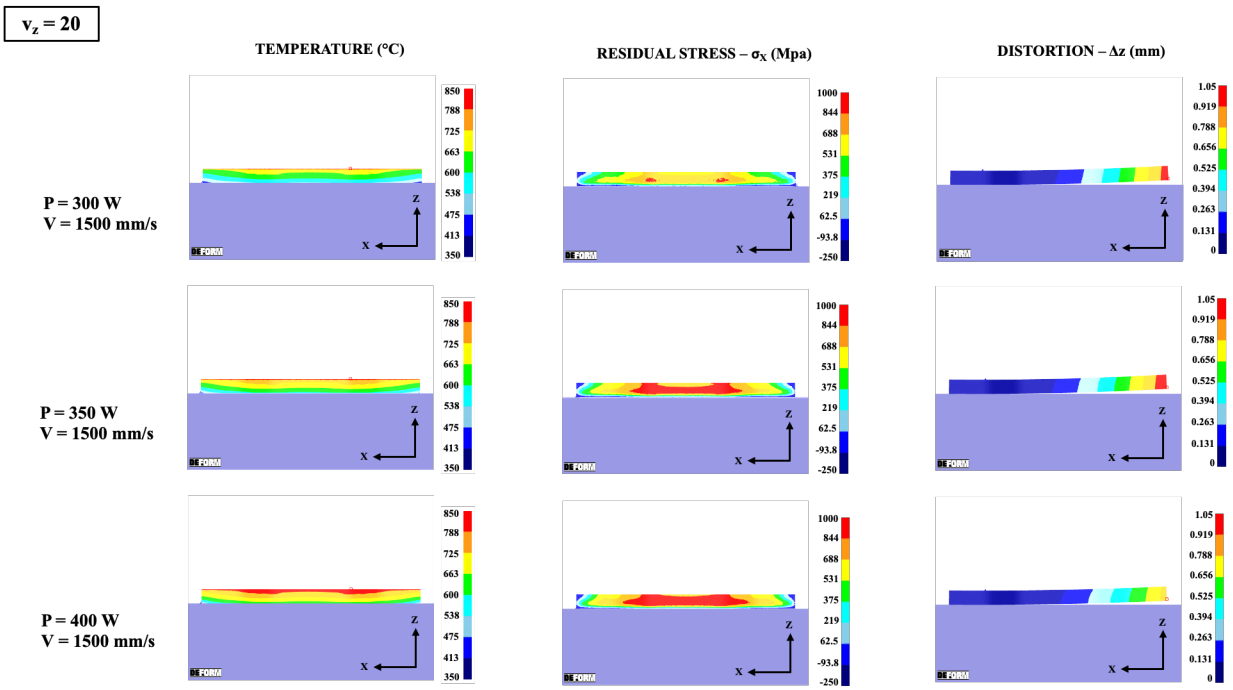

Fig. 4. Temperature profiles, residual stress profile, and distortion obtained from the numerical simulation with voxel mesh $v_z = 20$ and different laser power (300 W, 350 W, and 400 W).

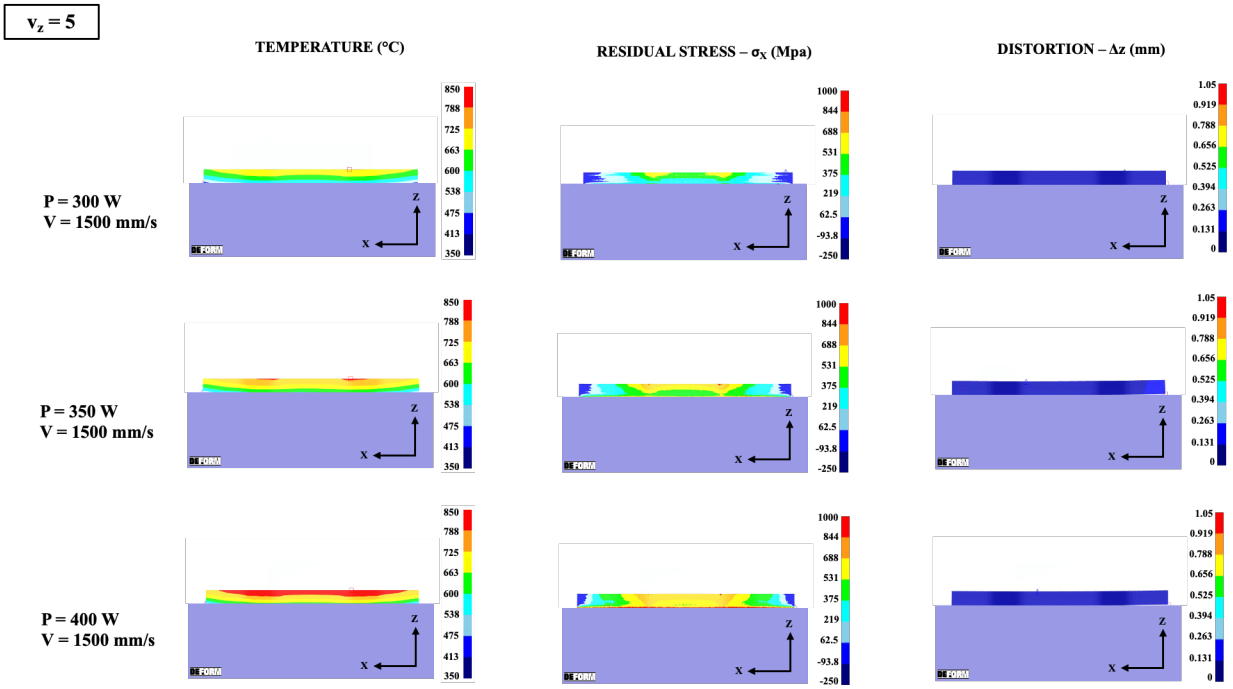

Fig. 5. Temperature profiles, residual stress profile, and distortion obtained from the numerical simulation with voxel mesh $v_z = 5$ and different laser power (300 W, 350 W, and 400 W).

In this way, the numerical model cannot reproduce with a good approximation the thermal exchange condition that occurs in the L-PBF process.

Fig. 5 shows how using $v_z = 5$ does not allow the correct development of residual stresses because there is no time for their development. The low residual stress values in fact result in almost no distortions.

Conclusions

In this paper, the commercial FEM software DEFORM 3D^{TM} whit a layer-by-layer approach was used to perform numerical simulations of the Ti-6Al-4V L-PBF process. The effect of laser power on residual stresses and part distortion was studied. Moreover, the model accuracy by varying the voxel mesh elements along the build direction was investigated. The main findings of this study can be summarized as follows:

- The laser power has a big impact on part distortion due to its influence on thermal gradients and residual stress profiles.
- The accuracy of the numerical model is strictly correlated to the number of voxel mesh elements used along the build direction.
- The number of real layers included in the computational ones decreases by increasing the number of voxel mesh elements in the build direction. This results in a better approximation of the L-PBF process.
- Using a few numbers of voxel mesh elements ($v_z = 5$) leads to the activation of several elements simultaneously without giving enough time for the residual stresses to develop.
- For the analyzed geometry, a good accuracy of the numerical model can be obtained only by employing 20 voxel mesh elements along the z-direction which results in a voxel mesh dimension of 0.15 mm.
- The best results in terms of model accuracy were obtained in the case of laser power P = 300 W when a $v_z = 20$ is considered.

Acknowledgments

This research was funded by Regione Sicilia under the scheme “Azione 1.2.1_03 del PO FESR SICILIA 2014-2020” – Progetto PON03 PE_00206_1 AMELIE ‘‘Advanced framework for Manufacturing Engineering and Product Lifecycle Enhancement.’’ CUP G76I20000060007.

References

[1] T. DebRoy, H.L. Wei, J.S. Zuback, T. Mukherjee, J.W. Elmer, J.O. Milewski, A.M. Beese, A. Wilson-Heid, A. De, W. Zhang, Additive manufacturing of metallic components – Process, structure and properties, Prog. Mater. Sci. 92 (2018) 112–224. https://doi.org/10.1016/j.pmatsci.2017.10.001

[2] G. Buffa, D. Palmeri, G. Pollara, F. Di Franco, M. Santamaria, L. Fratini, Process parameters and surface treatment effects on the mechanical and corrosion resistance properties of Ti6Al4V components produced by laser powder bed fusion, Progress in Additive Manufacturing (2023). https://doi.org/10.1007/s40964-023-00440-9

[3] S. Liu, Y.C. Shin, Additive manufacturing of Ti6Al4V alloy: A review, Mater. Des. 164 (2019) 8–12. https://doi.org/10.1016/j.matdes.2018.107552

[4] X. Lu, M. Chiumenti, M. Cervera, M. Slimani, I. Gonzalez, Recoater-Induced Distortions and Build Failures in Selective Laser Melting of Thin-Walled Ti6Al4V Parts, J. Manuf. Mater. Process. 7 (2023). https://doi.org/10.3390/jmmp7020064

[5] G. Buffa, A. Costa, D. Palmeri, G. Pollara, A. Barcellona, L. Fratini, A new control parameter to predict micro-warping-induced job failure in LPBF of TI6AL4V titanium alloy, Int. J. Adv. Manuf. Tech. 126 (2023). https://doi.org/10.1007/s00170-023-11179-6

[6] A. Razavykia, E. Brusa, C. Delprete, R. Yavari, An overview of additive manufacturing technologies-A review to technical synthesis in numerical study of selective laser melting, Materials 13 (2020) 1–22. https://doi.org/10.3390/ma13173895

[7] L. Bertini, F. Bucchi, F. Frendo, M. Moda, B.D. Monelli, Residual stress prediction in selective laser melting: A critical review of simulation strategies, Int. J. Adv. Manuf. Tech. 105 (2019) 609–636. https://doi.org/10.1007/s00170-019-04091-5

[8] E.L. Li, L. Wang, A.B. Yu, Z.Y. Zhou, A three-phase model for simulation of heat transfer and melt pool behaviour in laser powder bed fusion process, Powder Technol. 381 (2021) 298–312. https://doi.org/10.1016/j.powtec.2020.11.061

[9] M. Masoomi, S.M. Thompson, N. Shamsaei, Laser powder bed fusion of Ti-6Al-4V parts: Thermal modeling and mechanical implications, Int. J. Mach. Tool. Manuf. 118–119 (2017) 73–90. https://doi.org/10.1016/j.ijmachtools.2017.04.007

[10] N. Bastola, M.P. Jahan, N. Rangasamy, C.S. Rakurty, A Review of the Residual Stress Generation in Metal Additive Manufacturing: Analysis of Cause, Measurement, Effects, and Prevention, Micromachines (Basel) 14 (2023). https://doi.org/10.3390/mi14071480

[11] C. Chen, Z. Xiao, H. Zhu, X. Zeng, Deformation and control method of thin-walled part during laser powder bed fusion of Ti–6Al–4V alloy, Int. J. Adv. Manuf. Tech. 110 (2020) 3467–3478. https://doi.org/10.1007/s00170-020-06104-0

[12] D. Palmeri, G. Pollara, R. Licari, F. Micari, Finite Element Method in L-PBF of Ti-6Al-4V: Influence of Laser Power and Scan Speed on Residual Stress and Part Distortion, Metals (Basel) 13 (2023). https://doi.org/10.3390/met13111907